

# Numerical Study on Vortex Structures in a Two-dimensional Bluff-Body Burner in the Transitional Flow Regime

Hideo Kawahara <sup>1</sup> and Tatsuo Nishimura <sup>2</sup>

<sup>1</sup>Shipping Technology Department, Oshima National College of Maritime Technology,  
Oshima 742-2193 Japan

<sup>2</sup>Department of Mechanical Engineering, Yamaguchi University,  
Ube 755-8611 Japan

## ABSTRACT

Vortical structures are investigated numerically for both cold and combusting flows from a two-dimensional bluff-body burner in the transitional flow regime from steady to unsteady state. The Reynolds number of the central fuel flow is varied from 10 to 230 at a fixed air Reynolds number of 400. The flame sheet model of infinite chemical reaction and unit Lewis number are assumed in the simulation. The temperature dependence of the viscosity and diffusivity of the gas mixture is also considered. The vortex shedding is observed depending on the fuel flow. For cold flow, four different types of vortical structure are identified. However, for combusting flow of methane-air system the vortical structures change significantly due to a large amount of heat release during the combustion process, in contrast to cold flow.

**Keywords** : unsteady numerical simulation, non-premixed combustion, vortical structure, bluff-body burner.

## INTRODUCTION

Non-premixed combustion is stabilized by a bluff-body burner, such as occurs when a central fuel jet issues into a surrounding annular air jet, is often used industrially. Examples of the use of such burners are in the combustion chambers of gas turbines, tubular cooler, metallurgical furnaces, aircraft jet engines, etc. Such bluff-body burners provide good flame

stabilization as well as easy control of combustion. For non-premixed combustion in bluff-body burner, the stabilization mechanism is mainly controlled by the interaction among combustible mixtures, air flow and hot combustion products. Exchange of species, momentum and energy becomes more intensive due to the existence of unsteady recirculating structures behind bluff-body. Therefore, a completed understanding of flow field in

this region is very important for the study of flame stabilization. The influence of vortical shedding process on two dimensional bluff-body burner has been studied experimentally by Chin and Tankin [1-3]. In these studies, either under cold or combusting flow conditions, the detailed flow structures behind the bluff-body have been described. To capture the dynamic characteristics of the vortex shedding process, they used high-speed cameras. Through analysis of the films, flame-to-frame, detailed vortex movements were clearly detected. Furthermore, the vortical structures for cold flow conditions have been studied numerically by Chin and Tankin[3]. However they have not been studied numerically for combusting flow. In present study, we perform numerically cold and combusting flows in a two-dimensional bluff-body burner in the transitional flow regime.

## NUMERICAL SIMULATION

The numerical model employed in the present study is shown in Fig.1. The flow is time-dependent and two-dimensional. A Cartesian coordinates system is taken such that  $x$  is the streamwise direction,  $y$  is the transverse direction and the origin is the center of the fuel slot exit plane.  $u$  and  $v$  represent the streamwise and transverse velocity, respectively, and  $z$  is the coupling function. The boundary conditions for  $u$ ,  $v$  and  $z$  for the combusting flow are described in the figure. In the case cold flow, the boundary conditions in the analytical domain are given in a reference (Chin and Tankin[3]). The conservation equations for mass and momentum are given in the following forms.

$$\begin{aligned} & \frac{\partial p}{\partial t} + \frac{\partial}{\partial x} (\rho u) + \frac{\partial}{\partial y} (\rho v) + 0 \\ & \rho \left( \frac{\partial u}{\partial t} + u \frac{\partial u}{\partial x} + v \frac{\partial u}{\partial y} \right) = \\ & - \frac{\partial p}{\partial x} + \frac{4}{3} \frac{\partial}{\partial x} \left( \mu \frac{\partial u}{\partial x} \right) - \frac{2}{3} \frac{\partial}{\partial x} \left( \mu \frac{\partial v}{\partial y} \right) + \frac{\partial}{\partial y} \left[ \mu \left( \frac{\partial v}{\partial x} + \frac{\partial u}{\partial y} \right) \right] \\ & \rho \left( \frac{\partial v}{\partial t} + u \frac{\partial v}{\partial x} + v \frac{\partial v}{\partial y} \right) = \\ & - \frac{\partial p}{\partial y} + \frac{4}{3} \frac{\partial}{\partial y} \left( \mu \frac{\partial v}{\partial y} \right) - \frac{2}{3} \frac{\partial}{\partial y} \left( \mu \frac{\partial u}{\partial x} \right) + \frac{\partial}{\partial x} \left[ \mu \left( \frac{\partial u}{\partial y} + \frac{\partial v}{\partial x} \right) \right] \end{aligned}$$

Density is related to pressure  $p$ , temperature  $T$  and mass fraction  $Y_i$  through the following state equation

$$p = \rho R T \sum_{i=1}^4 (Y_i / m_i)$$

where  $m_i$  is the molecular weight of species  $i$  and  $R$  is the universal gas constant. The problem is further simplified by adopting the following coupling function  $z$ , i.e. Shvab-Zeldovich formulation:

$$z = \frac{Y_i - Y_{i,\infty}}{Y_{i,0} - Y_{i,\infty}} = \frac{Y - Y_\infty}{Y_0 - Y_\infty} = \frac{h - h_\infty}{h_0 - h_\infty}$$

where  $Y$  is given by

$$Y = (Y_F / m_F V_F) - (Y_O / m_O V_O)$$

and  $h$  is the sum of the thermal and chemical enthalpies. Suffix  $o$  denotes the value for the injected fuel, while  $\infty$  denotes the value for the co-flowing air stream. The energy conservation equation and the mass conservation equations for each species reduce to the following equation for  $z$ :

$$\rho \left( \frac{\partial z}{\partial t} + u \frac{\partial z}{\partial x} + v \frac{\partial z}{\partial y} \right) = \frac{\partial}{\partial x} \left( \rho D \frac{\partial z}{\partial x} \right) + \frac{\partial}{\partial y} \left( \rho D \frac{\partial z}{\partial y} \right)$$

The flame surface is located at the position where  $z$  becomes equal to  $Z_f$ , given by the equation:

$$Z_f = (Y_{O,\infty}/j) / (1 + (Y_{O,\infty}/j))$$

where  $j = m_o v_o / m_F v_F$ , i.e., mass of oxygen required to burn unit mass of fuel to attain complete combustion. The flame surface divides the whole region into two regions, i.e., fuel region inside the flame and air region outside the flame. The mass fractions and temperature in the respective regions can be written as follows for the when  $Y_{I,o} = 0$

Fuel region ( $1 > z > z_f$ )

$$Y_I = Y_{I,\infty}(1 - z)$$

$$T = T_\infty + (T_O - T_\infty)z + (q_O / m_F v_F C_p) j^{-1} Y_{O,\infty}(1 - z)$$

Air region ( $z_f > z > 0$ )

$$T = T_\infty + (T_O - T_\infty)z + (q_O / m_F v_F C_p) z$$

In the study, we shall adopt the following assumptions. The mixture undergoes an overall one-step irreversible reaction.

1. The reaction rate is infinitely fast and the reaction is concentrated within infinitesimally thin zone in the surface.
2. The mixture behaves like an ideal gas.
3. The soret and Dufour effects, as well as the pressure diffusion, can be neglected.
4. Specific heat at constant pressure of the mixture is constant.
5. The Lewis number is equal to unity.
6. Viscosity coefficient and diffusion coefficient depend on temperature.
7. In the energy equation viscous dissipation can be neglected.

The numerical calculation was performed by the finite-difference method. The scheme adopted here was the SIMPLE method[4].

The time differential and convective terms in the governing equations are treated with the implicit Euler scheme and QUICK scheme, respectively. The computational domain is  $0 < x < 14d$  and  $-5.5d < y < 5.5d$ . The grid numbers are  $91 \times 257$  non-uniform grid systems.

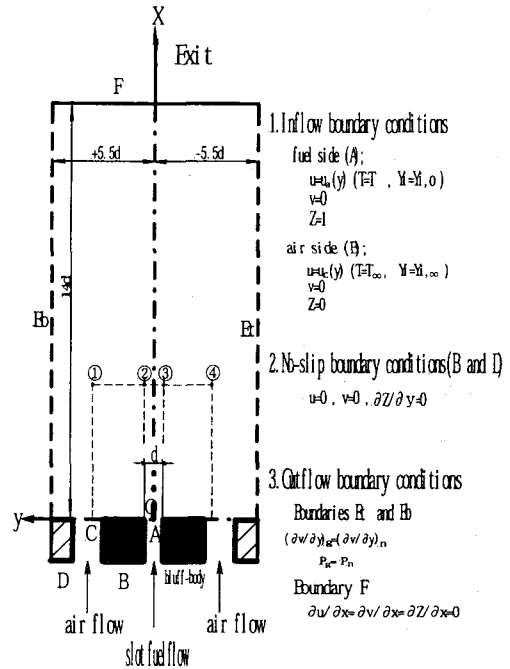


Fig.1 Computational flow domain and coordinates system.

## RESULT AND DISCUSSION

### Cold flow

Numerical calculations were performed by varying the Reynolds number for slot flow under a fixed Reynolds number for air flow, i.e.,  $Re_{slot} = 10-230$  and  $Re_{air} = 400$  to compare with the experimental results by Chin [1]. Four different types of vortical structures are predicted in the present calculation. Fig. 2 shows some numerical streakline patterns and the corresponding flow visualizations for type

2 and type 3. Agreement between calculated and observed streakline patterns are satisfactory. In type 2, inner and outer vortices are located on the bluff-body and they form a recirculating flow zone. Behind this zone, the vortices are weakly shed. In type 3, the vortical structure is more complicated and the recirculating flow zone is difficult to identify. The vortices are shed from the inner portion of the bluff-body and the shedding process is very clear.

Vortical shedding frequency is an important parameter in characterizing the instability of a

flow field. The shedding frequency was estimated from the velocity fluctuations at  $x/d=5$  and  $y/d=0.5$ . Fig. 3 shows the results of slot flow effect. The four regimes representing types of vortical structures are also presented in the figure. Although the shedding frequency increases with increasing the slot flow rate as a whole, there is a large jump in the frequency, i.e.,  $Re_{slot}=100-120$ , where a weak shedding process changes a strong one as shown in Fig. 2. The numerical results agree well with the experiments [1], at low slot flow rates.

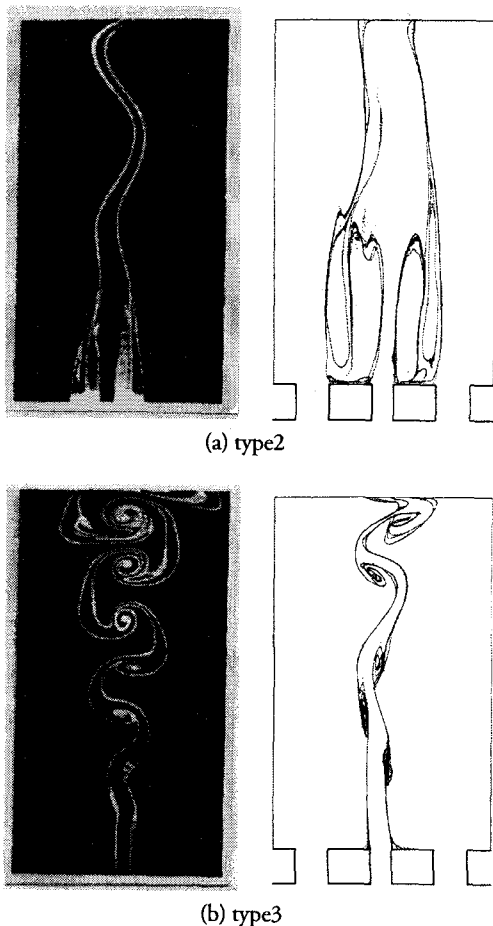


Fig. 2 Visualized photograph and simulated streakline patterns of vortical shedding for cold flow. (a) type 2; (b) type 3

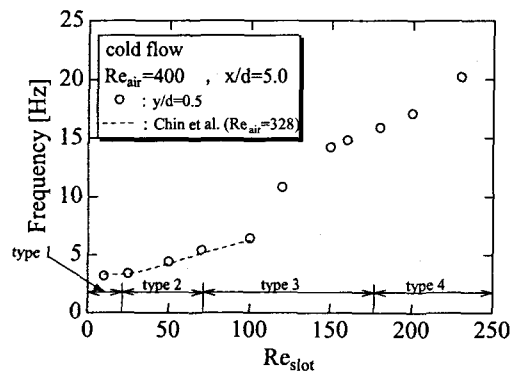


Fig. 3. Vortical shedding frequency vs. Re of slot flow for cold flow.

### Combusting flow

In the combustion system, methane ( $CH_4$ ) flows through the central slot burner and air flows outside, under the same hydrodynamical conditions as cold flow mentioned above. Heat release due to chemical reaction significantly alters the flow field. Fig. 4 shows several streakline patterns representing the typical flame and its vortical structures. For any fuel rate, there is a recirculating flow zone consisting of inner and outer vortices on the bluff-body, but the behavior of vortices strongly depends on the fuel rate. The flame attaches

to the outer portion of the bluff-body and it becomes unstable in the downstream part. In particular, flame deformation is remarkable in the fuel Reynolds number range of 70 to 150, i.e., a strong coupling of inner and outer vortices, indicating flame and vortex interaction.

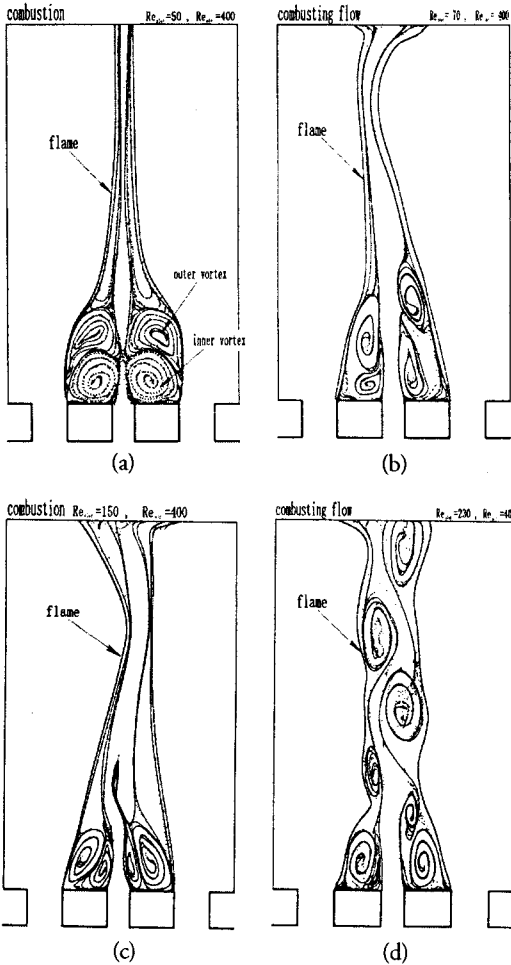


Fig.4 Simulated streakline patterns of vortical shedding for combustions. (a)  $Re_{slot}=50$  ; (b)  $Re_{slot}=70$  ; (c)  $Re_{slot}=150$  ; (d)  $Re_{slot}=230$

Fig. 5 shows several streamwise velocity fluctuations at two extreme cases, i.e.,  $Re_{slot}=50$  and 230. The measuring points (1,2,3,4) are

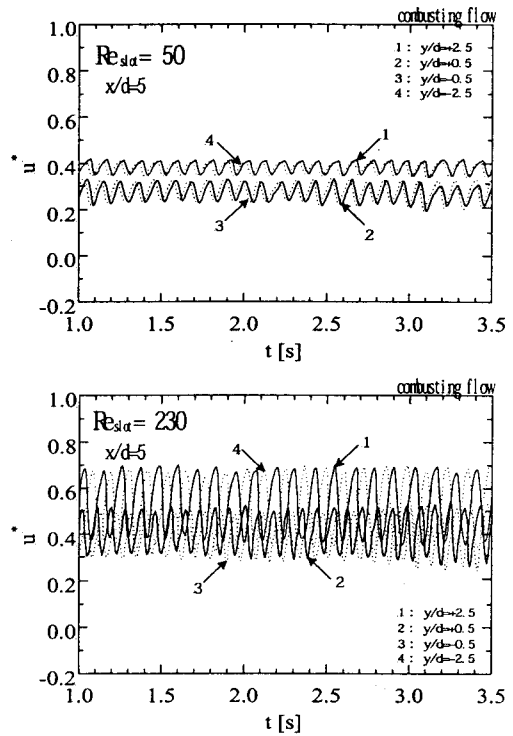


Fig.5 Time histories of four streamwise velocities for combustions.

located in air flow outside the flame and the points of 2 and 4 are located in fuel flow inside the flame. The amplitude and frequency of the velocity are almost identical both inside and outside the flame at  $Re_{slot}=50$ , but they are quite different at  $Re_{slot}=230$ , i.e., the frequency inside the flame is larger than that outside the flame. The effect of fuel flow rate on the frequency representing vortex shedding process is shown in Fig.6. In contrast to cold flow as shown in Fig.3, the frequency gradually decreases with increasing the fuel flow rate until  $Re_{slot}=150$ , where the trend is reverse above  $Re_{slot}=150$ . The frequency behavior for  $Re_{slot}<150$  is probably due to low fuel flow rates and suppression of the inner vortex in the presence of the flame. The whole tendency in the frequency coincides with the experi-

mental results by Chin [2]. Fig. 7 shows the corresponding amplitude effect. It is evident that the amplitude behavior does not correspond well to the frequency behavior. That is, the amplitude inside the flame increases with the fuel flow rate as a whole, but the amplitude effect is more complicated outside the flame. In particular, there is a large jump in the amplitude outside the flame at  $Re_{slot}=50-70$ , which suggests that the motion of outer vortex is enhanced due to the fuel penetration through the recirculating flow zone as shown in Fig.4. However, it should be noted that fur-

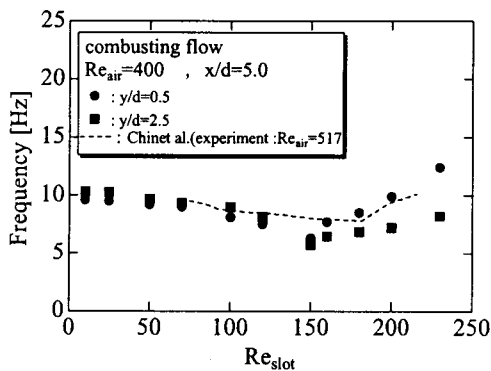


Fig. 6 Vortical shedding frequency vs.  $Re$  of slot flow for combustng flow.

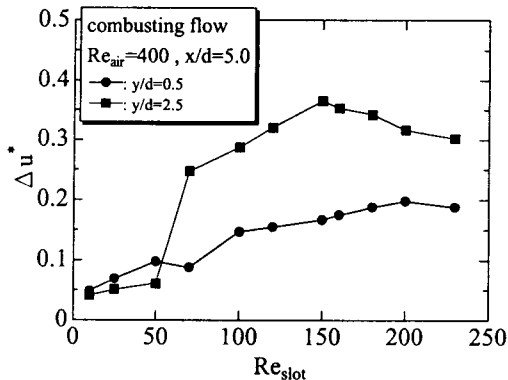


Fig. 7 Velocities amplitude vs.  $Re$  of slot flow for combustng flow.

ther increase of the fuel flow leads to suppression of the outer vortex, i.e.,  $Re_{slot}>150$ .

## CONCLUSIONS

We studied numerically the vortex structures of a two-dimensional bluff-body burner in the transitional flow regime. The conclusive remarks have been drawn as follows.

- 1) For cold flow, agreement between calculated and observed streakline patterns are satisfactory.
- 2) For combustng flow, there is a recirculating flow zone consisting of inner and outer vortices on bluff-body, and the behavior of vortices strongly depends on the fuel flow rate. In particular the vortex is differ the velocity fluctuations are quite different both inside and outside the flame at a high fuel flow rate

## REFERENCES

1. Chin, L. P., "Vortical Structures in 2-D Bluff-Body Burner", Ph.D thesis, Northwestern University, Evanston, Illinois (1990).
2. Chin, L. P. and Tankin, R. S., "Vortical Structures in a 2-D Vertical Bluff-Body Burner", *Combust.Sci.and Tech.*, Vol. 80, pp. 207-229 (1991).
3. Chin, L. P. and Tankin, R. S., "Vortical Structures from a Two-dimensional nozzle with a Bluff-Body Slot", *Phys. Fluids A4*(8), pp. 1724-1736 (1992).
4. Kawahara, H. and Nishimura, T., "Two-dimensional Simulation of Mathane/Air jet Diffusion Flames With/Without a Duct", *9<sup>th</sup> Int. Symposium on Flow Visualization*, CD-ROM No. 159 (2000).